JACS
JOURNAL OF THE AMERICAN CHEMICAL SOCIETY

ARTICLE

pubs.acs.org/JACS

Efficient Electron Transfer in a Protein Network Lacking Specific Interactions

Francesca Meschi,[†] Frank Wiertz,[‡] Linda Klauss,[‡] Anneloes Blok,[‡] Bernd Ludwig,[§] Angelo Merli,[†] Hendrik A. Heering,[‡] Gian Luigi Rossi,[†] and Marcellus Ubbink*[,‡]

[†]Department of Biochemistry and Molecular Biology, University of Parma, 43100 Parma, Italy

[‡]Institute of Chemistry, Leiden University, P.O. Box 9502, 2300 RA Leiden, The Netherlands

[§]Institute of Biochemistry, Molecular Genetics Group, and Cluster of Excellence Macromolecular Complexes, Goethe University, D-60438 Frankfurt, Germany

Supporting Information

ABSTRACT: In many biochemical processes, proteins need to bind partners amidst a sea of other molecules. Generally, partner selection is achieved by formation of a single-orientation complex with well-defined, short-range interactions. We describe a protein network that functions effectively in a metabolic electron transfer process but lacks such specific interactions. The soil bacterium *Paracoccus denitrificans* oxidizes a variety of compounds by channeling electrons into the main respiratory pathway. Upon conversion of methylamine by methylamine dehydrogenase, electrons are transported to the terminal oxidase to reduce molecular oxygen. Steady-state kinetic measurements and NMR experiments demonstrate a remarkable number of possibilities for the electron transfer, involving the cupredoxin amicyanin as well as four *c*-type cytochromes. The observed interactions appear to be governed exclusively by the electrostatic nature of each of the proteins. It is concluded that *Paracoccus* provides a pool of cytochromes for efficient electron transfer via weak, ill-defined interactions, in contrast with the view that functional biochemical interactions require well-defined molecular interactions. It is proposed that the lack of requirement for specificity in these interactions might facilitate the integration of new metabolic pathways.

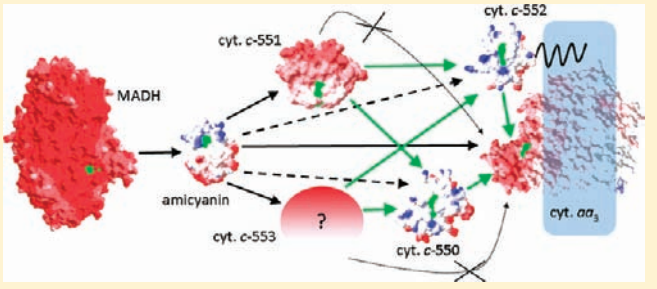

INTRODUCTION

The general view of protein interactions is that specificity is essential for biochemical processes to distinguish partners from nonpartners. In specific complexes, the proteins assume a single, well-defined orientation, stabilized by multiple short-range interactions, like salt bridges, H-bonds, van der Waals contacts and shielding of hydrophobic residues. In nonspecific complexes, proteins can assume multiple orientations. Electrostatic attraction between patches of charged residues on the proteins can stabilize nonspecific complexes and result in preorientation, creating preferred docking sites. However, the Coulombic force is a long-range interaction and on its own not sufficient to result in a specific complex. Many proteins are highly charged and, thus, such nonspecific complexes must be common, but these interactions are normally expected to have no biological function. Here, we report on a network of protein interactions that functions effectively in the transport of electrons, without a requirement for specificity.

The Gram-negative bacterium *Paracoccus denitrificans* can use methylamine (MA) as sole source of carbon and energy. The periplasmic enzyme MA dehydrogenase (MADH) converts this substrate to formaldehyde and ammonia and transfers the electrons to a small blue copper protein, amicyanin (ami).[1] From there, electrons eventually reach the terminal oxidase cytochrome aa_3 (cyt. aa_3), which reduces molecular oxygen to water. In the periplasmic space, three soluble *c*-type cytochromes[2,3] as well as a membrane-anchored one,[4] are also found, potentially all able to catalyze the electron transfer (ET) from ami to the oxidase. MADH, ami and cyt. *c*-551 were shown to crystallize in a ternary complex,[5] and on the basis of this result as well as kinetic data,[6] Davidson and co-workers proposed that ami is oxidized within the ternary complex. ET from cyt. *c*-551 to the membrane-bound oxidase was proposed to be mediated by cyt. *c*-550.[3] Recently, we showed that ami can reduce cyt. *c*-551, but only after dissociation from MADH, that is, in a ping-pong mechanism. We could not detect the ternary complex in solution.[7] The important role of the cytochromes in ET is not supported by a genetic study demonstrating that knockout of the genes encoding the three soluble *c*-type cytochromes, cyt. *c*-550, *c*-551, and *c*-553, does not prevent growth on MA.[8] Apparently, these cytochromes are not essential and various routes of ET are possible. We wondered

Received: June 1, 2011
Published: September 14, 2011

how promiscuous the proteins responsible for ET from MA to dioxygen are in their interactions. To address this question, the oxidation rate constants of ami by all possible partners, as well as most of the rates of ET among the cytochromes, were determined with an *in vitro* steady state reconstitution assay. The interaction of ami with all partners was also characterized with NMR spectroscopy. The pattern of reactivities shows that ET from ami involves a network of nonspecific protein complexes, rather than a defined chain of interactions. We discuss why the formation of specific complexes may be functionally unnecessary or even unfavorable for small ET proteins and speculate that having a pool of complementary cytochromes may represent an adaptive advantage for the bacterium.

RESULTS

Kinetics. To study the protein interactions involved in the transfer of electrons from ami to the terminal oxidase cyt. aa_3, steady-state electron transfer reactions were measured with an oxygraph. To an air-saturated solution containing MA in an oxygraph cell, cyt. aa_3 and MADH were added. No oxygen consumption was detected, showing that MA-reduced MADH cannot donate electrons directly to cyt. aa_3 for reduction of molecular oxygen. Addition of ami results in a constant decrease of the oxygen concentration in time, indicating that ami catalyzes the electron transfer from MADH to the oxidase, without the need for any *c*-type cytochromes. We reported this surprising finding recently in a previous paper.[7] In the absence of either MADH or cyt. aa_3, ami is not capable of oxygen reduction on the same time scale. The oxygen consumption depends nearly linearly on the amicyanin concentration up to at least 100 μM. The value of bimolecular rate constant k_2 is listed in Table 1, along with all other constants determined in the previous and in the present study for the MA-network, which is represented in Figure 1.

To establish which of the *c*-type cytochromes can reduce cyt. aa_3, the steady-state oxidation of each of the four reduced *c*-type cytochromes by cyt. aa_3 and oxygen was measured using a spectrophotometric assay. Cyt. *c*-550 and *c*-552 exhibit fast ET to cyt. aa_3, as expected from previous studies.[9,10] A linear fit to the concentration dependence (Figure S1) yields the rate constants k_4 and k_{11}, respectively. In contrast, cyt. *c*-551 and *c*-553 show no detectable ET to cyt. aa_3, in line with their reported inability to become oxidized by intact spheroplasts of *P. denitrificans*.[3]

To determine whether the *c*-type cytochromes can catalyze ET between ami and cyt. aa_3, the oxygraph assay was repeated in the presence of both ami and each of the *c*-type cytochromes. Figure 2 shows that cyt. *c*-551 and *c*-553 do not accelerate the reduction of oxygen, but rather have a slight inhibitory effect. An acceleration is not expected, because both cytochromes are unreactive toward the oxidase. The slight inhibition may be related to complex formation between ami and these cytochromes (see below).

Addition of either cytochrome *c*-550 or *c*-552 results in faster ET to the cyt. aa_3. Above a concentration of 5 μM, the increase in oxygen consumption is linear with increasing cytochrome concentration, yielding k_5^{app} and k_{12}^{app} for cyt. *c*-550 and *c*-552, respectively, because the rate-limiting step is the ET from ami to these cytochromes and not from the cytochromes to cyt. aa_3. The enhancement of the rate compared to that in the absence of these cytochromes appears to be large in Figure 2, but it should be noted that the concentration of the *c*-type cytochromes is up to 500-fold larger than the concentration of cyt. aa_3. Both rate constants are actually small, in the range of 10^3 M^{-1} s^{-1}, and about 50-fold lower than the rate for ET from ami directly to the oxidase (k_2). The value for k_5^{app} is close to what has been reported for the equivalent reaction for *Paracoccus versutus* proteins.[11] The small rate constants for the reduction of the cytochromes indicate that the interactions between ami and cyt. *c*-550 and *c*-552 are unfavorable.

Table 1. Reaction Parameters for the MA ET Network[a]

reaction	parameter	
MADH·ami → ami + MADH	k_1	26 ± 2 s^{-1} [b]
Ami + MADH → MADH·ami	k_{-1}	9 ± 2[b]
Ami → aa_3	k_2	0.17 − 0.26[b,c]
MADH → *c*-550	k_3	0.0039 (±0.0003)[b]
c-550 → aa_3	k_4	13 (±0.7)
Ami → *c*-550	k_5^{app}	0.0032 (±0.0001)
Ami → *c*-551	k_6	>k_7
c-551 → *c*-550	k_7	3.1 (±0.2)
Ami → *c*-553	k_8	>k_9
c-553 → *c*-550	k_9	0.66 (±0.05)
MADH → *c*-552	k_{10}	not determined
c-552 → aa_3	k_{11}	6.1 (±0.2)
Ami → *c*-552	k_{12}^{app}	0.0051 (±0.0002)
Ami → *c*-551	k_{13}	>k_{14}
c-551 → *c*-552	k_{14}	1.07 (±0.06)
Ami → *c*-552	k_{15}	>k_{16}
c-553 → *c*-552	k_{16}	0.183 (±0.009)
c-551 → aa_3		no ET detected
c-553 → aa_3		no ET detected
MADH·ami ⇌ ami + MADH (k_1/k_{-1})	K_d^{MA}	2.9 (±0.7)
MADH·*c*-550 ⇌ *c*-550 + MADH	K_d^{MC550}	40 (±6)[b]
Ami·aa_3 ⇌ ami + aa_3	$K_{d,app}^{Aaa3}$	12 (±1) (2:1)[d]
Ami·*c*-550 ⇌ ami + *c*-550	K_d^{AC550}	323 (±13)[d]
Ami·*c*-551 ⇌ ami + *c*-551	K_d^{AC551}	80 (±4)[b,d]
Ami·*c*-552 ⇌ ami + *c*-552	K_d^{AC552}	>1000[d]
Ami·*c*-553 ⇌ ami + *c*-553	$K_{d,app}^{AC553}$	58 (±3) (2:1)[d]

[a] The rate constants (k) are defined in Figure 1 and given in μM^{-1} s^{-1}, except for k_1. The dissociation constants (K_d) are given in μM. [b] Ref 7. [c] Some variation in k_2 was observed due to activity differences of the cyt. aa_3 in different experiments. [d] Determined from NMR titrations.

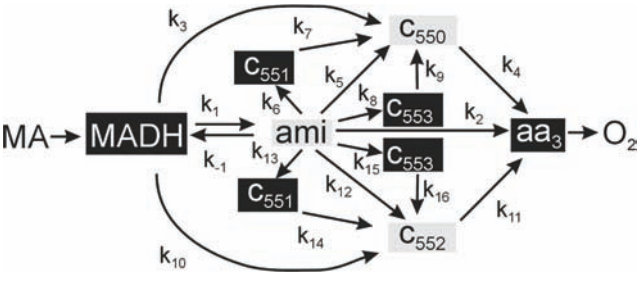

Figure 1. Schematic representation of the ET network for MA oxidation. The arrows indicate electron flow, with the *k* symbols referring to the reduction rate constants, except for k_1 and k_{-1}, which represent the dissociation and association rate constants of ami and MADH, respectively. The black and gray boxes denote negatively charged and dipolar proteins, respectively (see Discussion).

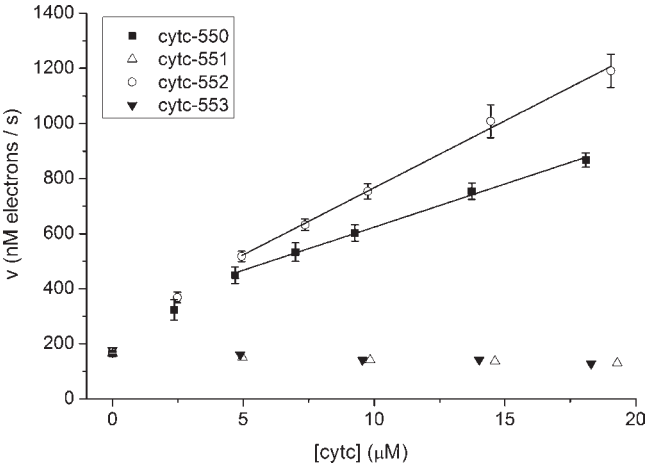

Figure 2. Steady-state ET from MA to dioxygen. The rate at 0 μM represents ET from ami to cyt. aa_3. Addition of cyt. *c*-550 and *c*-552, but not *c*-551 and *c*-553, enhances the rate. The solid lines represent linear fits. Conditions: ami, 10 μM; MADH, 200 nM (protomer concentration); cyt. aa_3, 40 nM; MA, 1 mM.

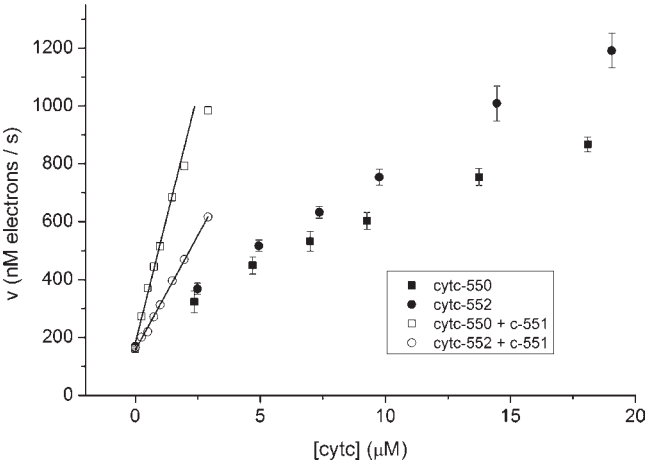

Figure 3. Steady-state ET from MA to dioxygen. The rate at 0 μM represents ET from ami to cyt. aa_3 and the solid symbols show the effect of the addition of either cyt. *c*-550 or *c*-552 only (data are the same as in Figure 2). The open circles show the effect of addition of cyt. *c*-550 or *c*-552 in the presence of 100 nM cyt. *c*-551. The solid lines represent linear fits yielding k_7 and k_{14}, respectively. For the cyt. *c*-550 + *c*-551 data set, the two points at highest cyt. *c*-550 concentration were not used in the fitting. Conditions: ami, 10 μM; MADH, 200 nM (protomer concentration); cytochrome aa_3, 40 nM; MA, 1 mM.

We then wanted to establish whether cyt. *c*-551 or *c*-553 could catalyze ET between ami and cyt. *c*-550 or *c*-552. We had reported before that cyt. *c*-551 enhances the ET to cyt. *c*-550[7] and this finding was reproduced in the current study. Furthermore, it was found that titrating either cyt. *c*-550 or *c*-552 into the oxygraph assay in the presence of ami and a fixed amount of cyt. *c*-551 (Figure 3) or *c*-553 (Figure S2) in all cases resulted in much faster oxygen consumption than without cyt. *c*-551 or *c*-553. Again, a linear increase in the rate is observed with increasing concentration of cyt. *c*-550/*c*-552, suggesting that ET from cyt. *c*-551/*c*-553 to cyt. *c*-550/*c*-552 (step 2) is rate limiting. This result implies that ET from ami to cyt. *c*-551/*c*-553 (step 1) is faster

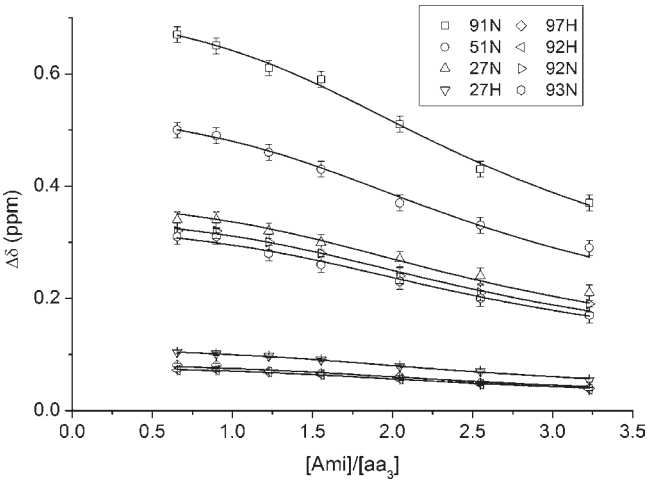

Figure 4. Binding curves for ami and cyt. aa_3. The chemical shift changes relative to those of free ami are plotted for the ratio of ami and cyt. aa_3. The solid lines represent a global fit to a 2:1 binding model with a single apparent dissociation constant of 12 μM. The residue number and observed amide nucleus are listed for each symbol. The error bars represent estimated experimental errors.

than step 2, despite the unfavorable free energies of these reactions (see below). Remarkably, all these rates are 3 orders of magnitude higher than those for the interactions of ami with cyt. *c*-550 and *c*-552, indicating that the interactions of ami with both cyt. *c*-551 and cyt. *c*-553 are much more favorable.

NMR Spectroscopy. The interactions between ami and the cytochromes were also studied using NMR spectroscopy. Per-deuterated and ^{15}N-labeled Zn(II)-ami was titrated into a solution of cyt. aa_3, resulting in chemical shift perturbations of the amide resonances in a TROSY spectrum. The copper in ami was substituted with Zn(II) to mimic the cupric form and avoid line broadening by ET and the paramagnetic nature of Cu(II). The binding curve (Figure 4) cannot be fitted well with a 1:1 binding model, but a model assuming a 2:1 stoichiometry for ami/cyt. aa_3 gives an excellent fit with a single, apparent dissociation constant ($K_{d,app}^{Aaa3}$) of 12 ($\pm$1) μM.

No perturbations were observed for ami in the MADH−ami complex upon addition of cyt. aa_3, indicating that the interaction between ami and cyt. aa_3 is lost when ami is bound to MADH (results not shown). Similarly, it has been observed that the interaction between ami and cyt. *c*-551 is lost upon complex formation of ami with MADH.[7] The binding site on ami for cyt. aa_3 is well-defined and comprises the so-called hydrophobic patch and surrounding positive residues, similar to the binding site for MADH and cyt. *c*-551 (Figure 5).[7,12]

The interaction of ami with the *c*-type cytochromes was studied by titrating the cytochrome into a solution of ^{15}N-labeled Zn(II)−ami. Cyt. *c*-550, *c*-552, and *c*-551 were in the reduced state, whereas cyt. *c*-553 was oxidized. The natural redox states would be reduced for ami and oxidized for the cytochromes, but the resulting ET would affect the NMR spectra negatively. Each of the cytochromes shows an interaction with ami, albeit with varying affinities. The binding curves are shown in Figure S3 and the K_d values are reported in Table 1. For cyt. *c*-550 and cyt. *c*-551,[7] a 1:1 binding curve fits the data well, whereas for cyt. *c*-553, a 2:1 (ami/cyt. *c*-553) model is required. The reason for this ratio is unclear, but cyt. *c*-553 is larger (22 kDa) than the other cytochromes. Its sequence has a single heme binding motif. Cyt.

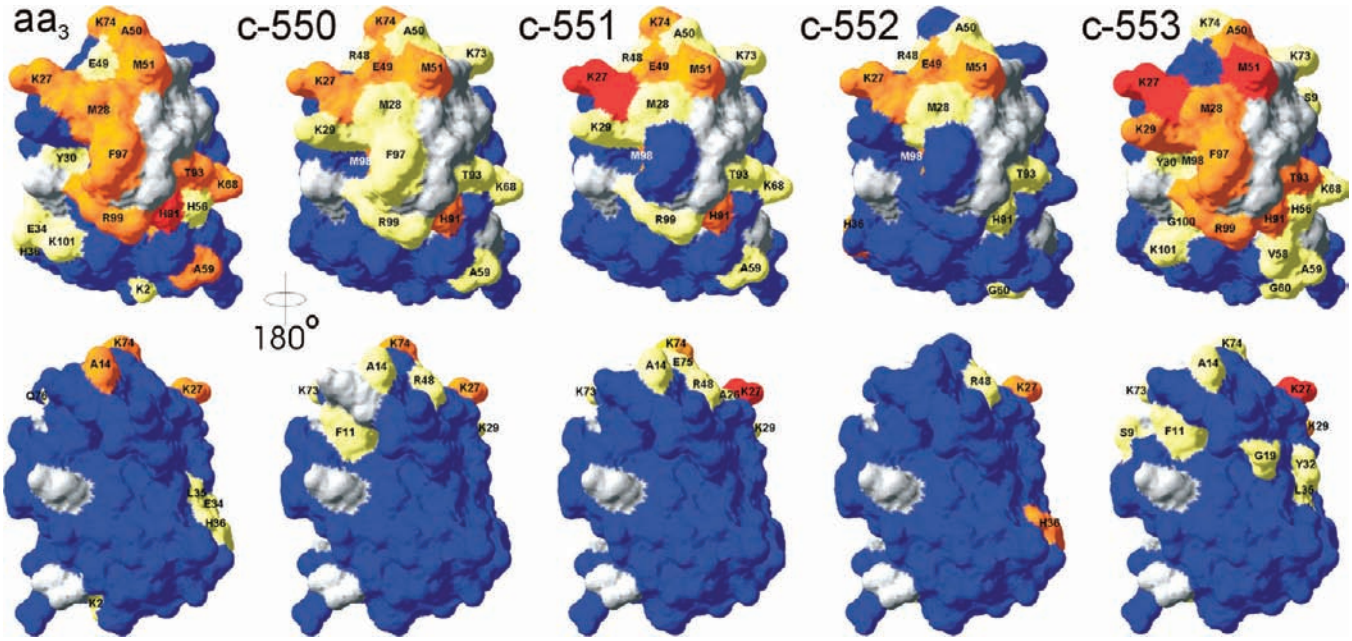

Figure 5. Binding maps for ami. The $\Delta\delta_{avg}$ (see Materials and Methods) was plotted on a surface representation of ami (PDB entry 1AAN[17]). $\Delta\delta_{avg}$ (ppm) > 0.1, red; $\Delta\delta_{avg}$ > 0.04 orange; $\Delta\delta_{avg}$ > 0.02 yellow; $\Delta\delta_{avg} \leq 0.02$, blue, except for cyt. c-552, for which $\Delta\delta_{avg} \leq 0.02$, orange, $\Delta\delta_{avg} \leq 0.01$ yellow and $\Delta\delta_{avg} \leq 0.006$, blue, were used; no data, gray. The data for cyt. *c*-551 have been taken from ref 7. In the bottom image, ami is rotated by 180° around the vertical axis in the plane, compared to the top image.

c-552 induces perturbations that are too small to be fitted reliably, suggesting a weak and dynamic interaction. The affinity for cyt. *c*-550 is low, whereas the interaction with cyt. *c*-551 and cyt. *c*-553 is in the normal range for transient electron transfer complexes.[13,14] The binding maps are shown in Figure 5. Clearly, ami uses the same surface area for the interaction with all the cytochromes. This finding suggests that ami does not bind to more than one partner simultaneously, consistent with a ping-pong mechanism of ET.[7]

Cyclic Voltammetry. To determine the driving forces for ET between ami and the *c*-type cytochromes, the midpoint potential was determined for all proteins as a function of pH. The results (Figure 6) show a very strong pH dependence for ami, in line with published work,[15] as a consequence of the change in copper coordination at low pH due to protonation of His 95. Also the data for the cytochromes can be fitted with protonation curves (Table S1), except for cyt. *c*-551, for which the potential shows a negligible pH dependence. At pH 7.5, used in the kinetic experiments, the midpoint potential difference (cyt. c − ami) is −1, −45, +38, and −85 mV for cyt. *c*-550, *c*-551, *c*-552, and *c*-553, respectively. Note that ET from ami to cyt. *c*-551 and, in particular, cyt. *c*-553 is uphill.

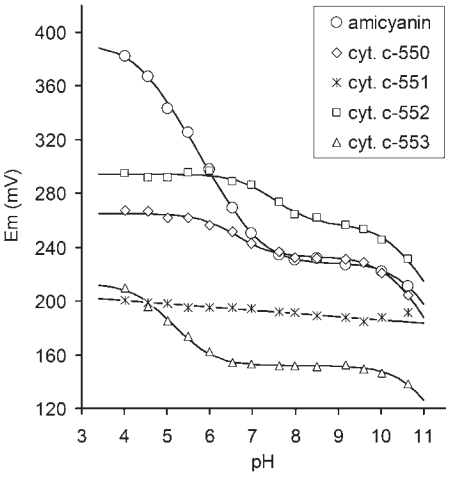

Figure 6. Midpoint potentials (Em) for ami and *c*-type cytochromes as a function of pH as determined by cyclic voltammetry. The solid lines represent fits of the data to eq S5. The fitted parameters are listed in Table S1. For cyt. *c*-551, no p*K* values could be resolved.

DISCUSSION

Our results indicate that electrons can flow from ami to cyt. aa_3 via several routes. Ami can form a transient complex with the oxidase, with an apparent 2:1 stoichiometry and an apparent affinity, at low ionic strength, in the low micromolar range. Ami reduces cyt. aa_3 with a rate that could well have physiological relevance. These findings are in accord with the genetic study by Van Spanning et al.[8] that demonstrated that *P. denitrificans* can still utilize MA as sole carbon and energy source in the absence of cyt. *c*-550, *c*-551, and *c*-553, although those authors suggested ET from ami to cyt. bc_1 and then to either cyt. cbb_3 or cyt. aa_3.[10,16] ET from ami to cyt. *c*-550 and *c*-552 is probably too slow to be of much importance physiologically, despite the fact that the driving forces for these reductions are not unfavorable.

In contrast, ET to cyt. *c*-553 and *c*-551 is fast, even though these reactions have positive free energy changes. The reactivities of the *c*-type cytochromes toward cyt. aa_3 are opposite to those toward ami. Cyt. *c*-550 and *c*-552, which are slowly reduced by ami, reduce the oxidase rapidly, whereas cyt. *c*-551 and *c*-553, that are rapidly reduced by ami, do not reduce cyt. aa_3. Consequently, apart from direct ET from ami to cyt. aa_3, only three-step ET from ami via cyt. *c*-551/*c*-553

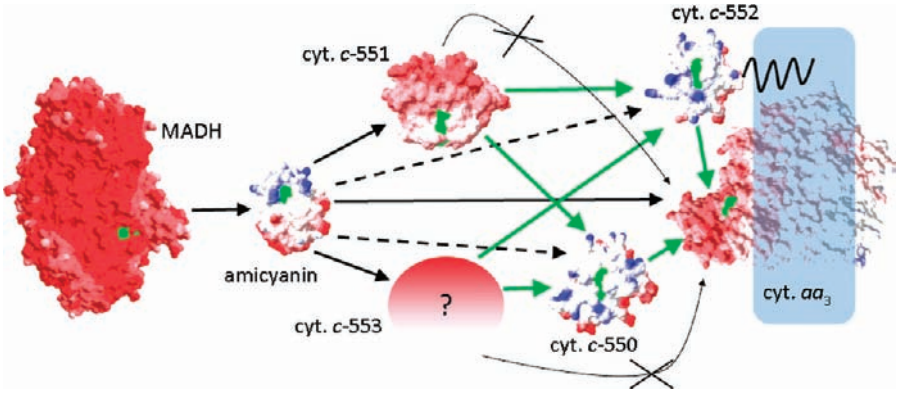

Figure 7. The MA ET network. The structures of the proteins studied in this work are shown in surface representation, colored according to surface charge. For MADH, cyt. *c*-551, and cyt. aa_3, the scale ranges from −12 to +12 au, and for ami and cyt. *c*-550 and *c*-552 from −4 to +4 au. Negative charges are in red, positive in blue. For cyt. *c*-553, no structure is available, but the sequence (UniProt entry P29967) indicates that it is a highly negative protein. The green areas mark the sites for strong electronic coupling to the redox center. Cyt. *c*-552 and cyt. aa_3 are depicted as integral membrane proteins. The black solid arrows indicate fast ET to or from ami. The dotted lines represent slow ET from ami, the green lines depict rapid ET between cytochromes, and the thin lines with a cross indicate that no ET was observed. PDB entries: MADH, 2BBK;[20] ami, 1AAN;[17] cyt. *c*-550, 155C;[21] cyt. *c*-551, 2MTA;[5] cyt. *c*-552, 1QL4;[22] cyt. aa_3, 3MK7.[23] Surface representations were produced using DeepView (Swiss-PdbViewer, http://spdbv.vital-it.ch/).

and *c*-550/*c*-552 to cyt. aa_3 is likely to contribute significantly to the flow of electrons (Figure 1).

It might appear as if the uphill reactions from ami to cyt. *c*-551/*c*-553 cannot be relevant for the oxidation of MA under physiological conditions. However, our experiments with the reconstituted redox chain show the opposite. The overall driving force for the reaction of MA and dioxygen to formaldehyde, ammonia, and water is very large (≈1 V). All the proteins in the redox chain are catalysts and, therefore, cannot alter the free energy change of this reaction. The uphill reaction from ami to cyt. *c*-551 or *c*-553 could only represent a kinetic barrier. However, a short distance between the copper and heme cofactors can be achieved in these small proteins, enabling an efficient electronic coupling and, thus, fast ET from ami to these cytochromes. In combination with rapid (downhill) ET from cyt. *c*-551/*c*-553 to cyt. *c*-550/*c*-552, the role of cyt. *c*-551/*c*-553 as ET mediators can still be effective, as also pointed out by Dutton and co-workers for other systems.[18]

Our finding that cyt. *c*-551 is the most reactive of the cytochromes toward ami is in agreement with earlier studies.[2] Compelling evidence indicates that it is free ami, not the ami-MADH complex, that transfers electrons to cyt. *c*-551.[7] However, it is clear that cyt. *c*-553 can replace cyt. *c*-551. Also cyt. *c*-550 and *c*-552 exhibit very similar properties in the ET reactions studied here. At least for the growth on MA, there appears to be redundancy in the available ET proteins, a finding that explains why single knockouts of the genes of the *c*-type cytochromes have a moderate[16] or no effect[8,10] on the growth of *P. denitrificans* on MA. However, nonredundant roles may exist for these cytochromes for ET from other donors. For example, genetic studies have shown that only cyt. *c*-551 can act as a partner for methanol dehydrogenase.[19] In this case, cyt. *c*-553 cannot act as a substitute.

The results of the current study suggest that ami can interact functionally with several proteins. ET from MADH to ami involves a specific, well-defined interaction, whereas ET from ami to cyt. aa_3 is best described by a network, rather than a chain, of protein interactions. The relative concentrations of the proteins are also important in determining the contribution of each branch of the ET network. On the basis of the protein yields from *P. denitrificans* cells, a crude estimation can be made about the relative concentrations and the electron fluxes (Supporting Information, Table S2 and Figure S4). In MA-cultured cells, the amount of cyt. *c*-553 is much lower than of MADH, ami, cyt. *c*-550, and cyt. *c*-551, which are found in approximately equal quantities. This estimation suggests that the ET flow through the ami−cyt. *c*-551−cyt. *c*-550−cyt. aa_3 route is dominant. However, the other interactions are functional and kinetically possible and thus can be expected to occur. The concept of a strictly defined linear pathway amidst a multitude of nonfunctional interactions is not applicable here. The relatively moderate reduction rates and binding affinities and the finding that the fastest reactions are uphill suggest that the network consists of protein interactions that have not been optimized by evolution. The binding site on ami is similar for all cytochromes and can therefore not be highly complementary to any one partner. Nevertheless, ET from ami to dioxygen is sufficiently fast to allow *P. denitrificans* to grow on MA. An analysis of the electrostatic properties of the proteins supports the view of an ET network dominated by electrostatic interactions. In Figure 7, the proteins are shown in surface representation, colored by charge. MADH, cyt. *c*-551, and the hydrophilic domain of subunit II of cyt. aa_3 are strongly negatively charged (red). Ami, cyt. *c*-550, and *c*-552 are dipolar, with the patch reactive in ET (green) in the positively charged (blue) hemisphere of the protein. For cyt. c-553, no structure is available, but the sequence contains nearly twice more negative than positive residues. Ami reacts fast with proteins that have a negative reaction patch and slowly with cyt. *c*-550 and *c*-552.

Similarly, the negative *c*-type cytochromes react rapidly with those with positive reactive patches and not with the other negative proteins. Thus, electrostatic attraction and repulsion between the partners alone is sufficient to explain the observed pattern of reactivity. The rate of ET depends on the driving force, the reorganization energy, and the electronic coupling between the redox centers.[24] The driving force and reorganization energy are not significantly influenced by complex formation, but the electronic coupling depends strongly on the interaction between the proteins. In large ET complexes, a specific state is required, in which the redox centers are brought close enough to allow for sufficient electron coupling and, thus, fast ET.[25] For complexes of small electron transfer proteins like ami and the *c*-type cytochromes, it is possible to achieve very efficient electronic coupling by

Table 2. Potential Monoheme *c*-Type Cytochromes in *P. denitrificans* Pd1222 (http://genome.jgi-psf.org/parde/parde.home.html)

genome locus	name	size (aa) mature protein	genetic neighborhood
0021	*c*-553	198	XDH
1808	*c*-552	148	
1937	*c*-550	134	
2307	c_1	425	Cyt. *c* reductase subunits
2489	*c*-55x	86	Nitrogen metabolism
2544		131	Cobyrinate synthesis
2995	*c*-551	154	Methanol oxidation
3238		130	
4150	SoxX	133	Sulfur oxidation
4700		131	Acriflavin resistance

bringing the redox centers in close proximity. The favorable electrostatic interactions can ensure that such positioning occurs in a large fraction of the encounters of two proteins.[26,27] A well-defined single orientation, as observed in specific protein−protein complexes, is not required in small ET protein complexes and may even be unfavorable, because it could result in lower turnover rates.[25,28−30] Thus, a network of electrostatic interactions is sufficient to transfer electrons quickly and effectively down the free energy gradient.

This observation poses the question whether there could be an evolutionary advantage to produce several *c*-type cytochromes with similar properties, capable of forming electrostatically favored, but nonspecific, complexes with other proteins. The genome of *P. denitrificans* strain Pd1222 has been sequenced. Table 2 lists the proteins likely to be monoheme *c*-type cytochromes. The genes are spread over the genome, with separate promoters and most are located close to possible partner redox enzymes. Cyt. *c*-551 and *c*-553 are induced simultaneously, probably by formaldehyde,[31] a common intermediate in the metabolism of various C1 compounds. Cyt. *c*-550 appears to be constitutively expressed.[31] In our cultures grown on MA, we found three soluble cytochromes, so it is assumed that the other soluble *c*-type cytochromes are expressed only under different conditions.

We speculate that such a pool of ET proteins makes it possible to 'plug-in' new metabolic routes. When the genes for enzymes capable of oxidizing a particular substrate are acquired via lateral gene transfer, as appears to be very common among bacteria,[32] the minimal requirement to benefit from such an acquisition is the need to transfer the electrons to a terminal oxidase. The pool of *c*-type cytochromes ensures that the electrons will be transferred one way or another. We note that the entire set of genes for MA growth is encoded by a single stretch of DNA (*mau* operon), including the gene for ami and the genes required for the processing of MADH and its TTQ-cofactor.[33−37] This set might simply have been acquired from another bacterium. Such a 'plug-and-grow' mechanism would be highly beneficial for a nonmotile soil bacterium like *P. denitrificans* that may be confronted with strongly varying conditions, requiring metabolic versatility.

MATERIALS AND METHODS

Protein Preparation. The purification of MADH, ami, cyt. *c*-550, cyt. *c*-551, and cyt. aa_3 from *P. denitrificans* has been reported before.[7] Cyt. *c*-553 was obtained with the same protocol as cyt. *c*-551, with the proteins eluting in different fractions. The soluble domain of cyt. *c*-552 was prepared as published.[9] The production of isotope-labeled Zn(II)−ami followed the reported procedure.[7]

Activity Assays. Kinetic assays were performed at 20 °C in 1 mM MA hydrochloride, 10 mM potassium phosphate (pH 7.5), 50 mM KCl, 1 mM EDTA, and 0.1%, dodecyl maltoside. Oxygen consumption was measured with a Hansatech Instruments oxygraph equipped with a Clark electrode. The oxygraph was calibrated with sodium dithionite and the reaction volume was 400 μL. The rate of oxygen consumption was determined by measuring the slope of concentration decrease. A Varian Cary 50 UV−vis spectrophotometer was used to measure the steady-state oxidation rate of the cytochromes by cyt. aa_3. Cytochromes were reduced with sodium ascorbate and applied to a PD-10 desalting column (GE Healthcare) to remove the ascorbate. The reaction volume was 100 μL and the reaction was initiated by the addition of cyt. aa_3. Errors were set to the SD of duplicate experiments or estimated from the experimental measurements and propagated. Errors of the protein concentrations were estimated to be 5%. The models for the kinetic analysis are described in the Supporting Information.

NMR Titrations. NMR experiments were performed at 300 K on a Bruker Avance DMX 600 MHz NMR spectrometer equipped with a TCI-Z-GRAD ATM cryoprobe. All solutions contained 20 mM Hepes (pH 7.6) and 6% D_2O. For samples containing cyt. aa_3, 0.1%, dodecyl maltoside was added. TROSY spectra were recorded during the inverse titration of a 70 μM cyt. aa_3 sample with a 0.9 mM stock solution of $^{15}N-^{2}H-Zn(II)$−ami. For the *c*-type cytochrome titration experiments, a series of $^{15}N-^{1}H$ HSQC and 1D spectra of a 100 μM $^{15}N-Zn(II)$−ami sample with increasing concentrations of cytochromes was recorded. All cytochromes had been reduced with sodium ascorbate, except for cyt. *c*-553 which had been oxidized with $K_3Fe(CN)_6$. Data processing and analysis of the chemical shift perturbations, including the definition of $\Delta\delta_{avg}$, followed the published procedure,[7] except that a correction factor of 2 for the cytochrome concentration was introduced for fitting the binding curves of ami with cyt. aa_3 and cyt. *c*-553, to account for a 2:1 binding ratio.

Cyclic Voltammetry. The reduction potentials of ami, cyt. *c*-550, cyt. *c*-551, cyt. *c*-552 (soluble domain), and cyt. *c*-553 were determined by cyclic voltammetry. The proteins were diluted to 69, 26, 16, 63, and 14 μM, respectively, in 90 mM of buffer (citric acid, MES, MOPS, TAPS, or CAPS, titrated with NaOH to the desired pH between 4.0 and 10.6). The working electrode was a 3.1 mm^2 gold electrode (CH-instruments), polished with suspensions of 1 μm, 0.3 μm, and 50 nm alumina on microcloth (Buehler), sonicated in water, subsequently incubated for at least 2 h in 1 mM aqueous mercaptohexanol (Sigma), and rinsed thoroughly with water. The working electrode was mounted on a glass microliter cell as described by Hagen,[38] modified to accommodate the CHI working electrode, and equipped with a water jacket connected to a refrigerated circulating water bath (VWR) at constant temperature of 24 °C. The reference electrode was a saturated calomel electrode (SCE, Radiometer REF401), and the counter electrode was a Pt wire. The electrodes were connected to an Autolab PGstat12 potentiostat (Metrohm), controlled by GPES 4.9 software. A 20 μL droplet of buffered protein solution was suspended between the three electrodes, the cell headspace was flushed with Ar, and staircase cyclic voltammograms were recorded with a step size of 2 mV at a scan rate of 10 mV/s (20 mV/s for ami, 5 mV/s for cyt. *c*-550), where the responses are (nearly) ideally reversible. The midpoint potentials were determined by averaging the oxidative and reductive peak positions of four cycles, and converted to the standard hydrogen electrode scale by adding the SCE potential of 245 mV at 24 °C.[39]

ASSOCIATED CONTENT

Supporting Information. Kinetic models, details of the cyclic voltammetry, additional kinetic data and NMR binding

curves. This material is available free of charge via the Internet at http://pubs.acs.org.

AUTHOR INFORMATION

Corresponding Author
m.ubbink@chem.leidenuniv.nl

ACKNOWLEDGMENT

F.W., H.A.H. and M.U. were supported by The Netherlands Organization for Scientific Research (NWO), VIDI grant 700.53.424 (F.W. and H.A.H.) and VICI grant 700.58.441 (M.U.). The Parma group was supported by the Ministry of University and Research, MIUR, Grant PRIN 20074TJ3ZB_004. B.L. acknowledges the support of DFG (SFB472 and CEF-MC, Project EXC 115).

REFERENCES

(1) Husain, M.; Davidson, V. L. *J. Biol. Chem.* **1985**, *260*, 4626–4629.
(2) Husain, M.; Davidson, V. L. *J. Biol. Chem.* **1986**, *261*, 8577–8580.
(3) Davidson, V. L.; Kumar, M. A. *FEBS Lett.* **1989**, *245*, 271–273.
(4) Turba, A.; Jetzek, M.; Ludwig, B. *Eur. J. Biochem.* **1995**, *231*, 259–265.
(5) Chen, L.; Durley, R. C.; Mathews, F. S.; Davidson, V. L. *Science* **1994**, *264*, 86–90.
(6) Davidson, V. L.; Jones, L. H. *J. Biol. Chem.* **1995**, *270*, 23941–23943.
(7) Meschi, F.; Wiertz, F.; Klauss, L.; Cavalieri, C.; Blok, A.; Ludwig, B.; Heering, H. A.; Merli, A.; Rossi, G. L.; Ubbink, M. *J. Am. Chem. Soc.* **2010**, *132*, 14537–14545.
(8) van Spanning, R. J. M.; Wansell, C. W.; Reijnders, W. N. M.; Harms, N.; Ras, J.; Oltmann, L. F.; Stouthamer, A. H. *J. Bacteriol.* **1991**, *173*, 6962–6970.
(9) Reincke, B.; Thony-Meyer, L.; Dannehl, C.; Odenwald, A.; Aidim, M.; Witt, H.; Ruterjans, H.; Ludwig, B. *Biochim. Biophys. Acta, Bioenerg.* **1999**, *1411*, 114–120.
(10) Otten, M. F.; van der Oost, J.; Reijnders, W. N. M.; Westerhoff, H. V.; Ludwig, B.; van Spanning, R. J. M. *J. Bacteriol.* **2001**, *183*, 7017–7026.
(11) Ubbink, M.; Hunt, N. I.; Hill, H. A.; Canters, G. W. *Eur. J. Biochem.* **1994**, *222*, 561–571.
(12) Chen, L.; Durley, R.; Poliks, B. J.; Hamada, K.; Chen, Z.; Mathews, F. S.; Davidson, V. L.; Satow, Y.; Huizinga, E.; Vellieux, F. M. *Biochemistry* **1992**, *31*, 4959–4964.
(13) Crowley, P. B.; Ubbink, M. *Acc. Chem. Res.* **2003**, *36*, 723–730.
(14) Prudencio, M.; Ubbink, M. *J. Mol. Recogn.* **2004**, *17*, 524–539.
(15) Zhu, Z. Y.; Cunane, L. M.; Chen, Z. W.; Durley, R. E.; Mathews, F. S.; Davidson, V. L. *Biochemistry* **1998**, *37*, 17128–17136.
(16) van Spanning, R. J. M.; Wansell, C.; Harms, N.; Oltmann, L. F.; Stouthamer, A. H. *J. Bacteriol.* **1990**, *172*, 986–996.
(17) Durley, R.; Chen, L. Y.; Mathews, F. S.; Davidson, V. L. *Protein Sci.* **1993**, *2*, 739–752.
(18) Page, C. C.; Moser, C. C.; Chen, X. X.; Dutton, P. L. *Nature* **1999**, *402*, 47–52.
(19) van Spanning, R. J. M.; Wansell, C. W.; de Boer, T.; Hazelaar, M. J.; Anazawa, H.; Harms, N.; Oltmann, L. F.; Stouthamer, A. H. *J. Bacteriol.* **1991**, *173*, 6948–6961.
(20) Chen, L. Y.; Doi, N.; Durley, R. C. E.; Chistoserdov, A. Y.; Lidstrom, M. E.; Davidson, V. L.; Mathews, F. S. *J. Mol. Biol.* **1998**, *276*, 131–149.
(21) Timkovich, R.; Dickerson, R. E. *J. Biol. Chem.* **1976**, *251*, 4033–4046.
(22) Harrenga, A.; Reincke, B.; Ruterjans, H.; Ludwig, B.; Michel, H. *J. Mol. Biol.* **2000**, *295*, 667–678.
(23) Koepke, J.; Olkhova, E.; Angerer, H.; Muller, H.; Peng, G. H.; Michel, H. *Biochim. Biophys. Acta, Bioenerg.* **2009**, *1787*, 635–645.
(24) Marcus, R. A.; Sutin, N. *Biochim. Biophys. Acta* **1985**, *811*, 265–322.
(25) Bashir, Q.; Volkov, A. N.; Ullmann, G. M.; Ubbink, M. *J. Am. Chem. Soc.* **2010**, *132*, 241–247.
(26) Ubbink, M. *FEBS Lett.* **2009**, *583*, 1060–1066.
(27) Schreiber, G.; Haran, G.; Zhou, H. X. *Chem. Rev.* **2009**, *109*, 839–860.
(28) Xu, X. F.; Reinle, W. G.; Hannemann, F.; Konarev, P. V.; Svergun, D. I.; Bernhardt, R.; Ubbink, M. *J. Am. Chem. Soc.* **2008**, *130*, 6395–6403.
(29) Xiong, P.; Nocek, J. M.; Griffin, A. K. K.; Wang, J. Y.; Hoffman, B. M. *J. Am. Chem. Soc.* **2009**, *131*, 6938–6939.
(30) Liang, Z. X.; Jiang, M.; Ning, Q.; Hoffman, B. M. *J. Biol. Inorg. Chem.* **2002**, *7*, 580–588.
(31) Baker, S. C.; Ferguson, S. J.; Ludwig, B.; Page, M. D.; Richter, O. M. H.; van Spanning, R. J. M. *Microbiol. Mol. Biol. Rev.* **1998**, *62*, 1046–1078.
(32) Treangen, T. J.; Rocha, E. P. C. *PLoS Genet.* **2011**, *7*, e1001284.
(33) Chistoserdov, A. Y.; Boyd, J.; Mathews, F. S.; Lidstrom, M. E. *Biochem. Biophys. Res. Commun.* **1992**, *184*, 1181–1189.
(34) van der Palen, C. J. N. M.; Slotboom, D. J.; Jongejan, L.; Reijnders, W. N. M.; Harms, N.; Duine, J. A.; van Spanning, R. J. M. *Eur. J. Biochem.* **1995**, *230*, 860–871.
(35) Delorme, C.; Huisman, T. T.; Reijnders, W. N. M.; Chan, Y. L.; Harms, N.; Stouthamer, A. H.; van Spanning, R. J. M. *Microbiology* **1997**, *143*, 793–801.
(36) van der Palen, C. J. N. M.; Reijnders, W. N. M.; deVries, S.; Duine, J. A.; van Spanning, R. J. M. *Antonie van Leeuwenhoek* **1997**, *72*, 219–228.
(37) van Spanning, R. J. M.; Wansell, C. W.; Reijnders, W. N. M.; Oltmann, L. F.; Stouthamer, A. H. *FEBS Lett.* **1990**, *275*, 217–220.
(38) Hagen, W. R. *Eur. J. Biochem.* **1989**, *182*, 523–530.
(39) Bard, A. J.; Faulkner, L. R. *Electrochemical Methods: Fundamentals and Applications*; Wiley & Sons: New York, 2001.